

Novel Pb and Zn Coordination Polymers: Synthesis, Molecular Structures, and Third-Order Nonlinear Optical Properties

Xiangru Meng,[†] Yinglin Song,[‡] Hongwei Hou,^{*†} Yaoting Fan,[†] Gang Li,[†] and Yu Zhu[†]

Department of Chemistry, Zhengzhou University, Zhengzhou 450052, Henan, P. R. China, and
Department of Physics, Harbin Institute of Technology, Heilongjiang 150001, P. R. China

Received August 3, 2002

Three novel coordination polymers $[\text{Pb}(\text{bbbm})_2(\text{NO}_3)_2]_n$ (bbbm = 1,1'-(1,4-butanediyl)bis-1*H*-benzimidazole) **1**, $[\text{Zn}(\text{bbbt})(\text{NCS})_2]_n$ (bbbt = 1,1'-(1,4-butanediyl)bis-1*H*-benzotriazole) **2**, and $[\text{Zn}(\text{pbbt})(\text{NCS})_2]_n$ (pbbt = 1,1'-(1,3-propylene)bis-1*H*-benzotriazole) **3** were synthesized and structurally characterized. Polymer **1** exhibits a two-dimensional rhombohedral grid network structure, the dimensions of the grid are $14.274 \times 14.274 \text{ \AA}$, and the diagonal-to-diagonal distances are $24.809 \times 14.125 \text{ \AA}$. Polymer **2** possesses a concavo-convex chain structure different from those of the known one-dimensional polymers, which are linear chain, zigzag chain, helical chain, double-stranded chain, and ladder chain. Polymer **3** exhibits a one-dimensional zigzag chain structure, and these chains were packed as an ...ABAB... layered structure. The third-order nonlinear optical (NLO) properties of polymers **1**, **2**, and **3** were determined with a 7-ns pulsed laser at 532 nm. **1** shows strong third-order NLO absorptive and refractive properties, and its α_2 and n_2 values were calculated to be $5.8 \times 10^{-9} \text{ m W}^{-1}$ and $4.67 \times 10^{-18} \text{ m}^2 \text{ W}^{-1}$ in a $3.4 \times 10^{-4} \text{ mol dm}^{-3}$ DMF solution, respectively. Both **2** and **3** exhibit weaker NLO absorption and strong refractive properties, and their n_2 values are $4.53 \times 10^{-18} \text{ m}^2 \text{ W}^{-1}$ for **2** in a $5.2 \times 10^{-4} \text{ mol dm}^{-3}$ DMF solution and $3.02 \times 10^{-18} \text{ m}^2 \text{ W}^{-1}$ for **3** in a $4.35 \times 10^{-4} \text{ mol dm}^{-3}$ DMF solution. The $\chi^{(3)}$ values of **1**, **2**, and **3** were calculated to be 1.67×10^{-11} , 1.62×10^{-11} , and $1.08 \times 10^{-11} \text{ esu}$, respectively, and the values are larger than those of the reported coordination polymers. We deduce that the valence shell structures of metal ions may have some influence on the strength of NLO properties, and discuss the relationships between the crystal structures of coordination polymers and the observed NLO properties.

Introduction

The design and synthesis of new materials with large macroscopic nonlinearities has been receiving more and more attention as it represents an active research field in modern chemistry, physics, and materials science.¹ To date, people have synthesized many nonlinear optical materials which possess commercial device applications, optical phase conjugation and image processing, optical switching, optical data processing, new frequency generation, etc.² Among these,

the best performing materials reported in the literature are conjugated organic polymers, organometallic compounds, fullerenes, semiconductors, and clusters, such as polythiophene, ferrocene derivatives, C_{60} , C_{70} , GaAs, Ge, $[\text{MoOS}_3\text{Cu}_3(\text{SCN})(\text{Py})_5]$, and $\{[\text{Et}_4\text{N}]_2[\text{WS}_4\text{Cu}_4(\text{CN})_4]\}_n$, etc.³ It is well-known that coordination polymers play an important role in the family of nonlinear optical materials.⁴

Furthermore, the design and self-assembly of coordination polymers with novel structures is attractive due to their special properties, such as electrical conductivity, magnetism, host–guest chemistry, and catalysis.⁵ So far most of the coordination polymers are formed by rigid ligands and have relatively large voids and potential interest for guest–host interaction and molecular recognition. Treatment of 2,4,6-tri(1-imidazolyl)-1,3,5-triazine and zinc bromide affords a

* Author to whom correspondence should be addressed. E-mail: houhongw@zzu.edu.cn.

[†] Zhengzhou University.

[‡] Harbin Institute of Technology.

(1) (a) Marks, T. J.; Ratner, M. A. *Angew. Chem., Int. Ed. Engl.* **1995**, *34*, 155. (b) Marder, S. R.; Sohn, J. E.; Stucky, G. D. *Materials for Nonlinear Optics*; ACS Symposium Series 455; American Chemical Society: Washington, DC, 1991. (c) Keller, O. *Nonlinear Optics in Solids*; Proceedings International Summer School; Springer: Berlin, 1990. (d) Lyons, M. H. *Materials for Nonlinear and Electrooptics*; Institute of Physics Conference Series 103; Institute of Physics: Bristol, 1989.

(2) (a) Long, N. J. *Angew. Chem., Int. Ed. Engl.* **1995**, *34*, 21. (b) Karna, S. P.; Yeates, A. T. *Nonlinear Optical Material*; American Chemical Society: Washington, DC, 1996. (c) Shi, S. *Contemp. Phys.* **1994**, *35*, 21.

large-pore zeotype coordination polymer.⁶ Layering a MeOH solution of Ni(NO₃)₂·6H₂O onto a benzene solution of 1,4-bis(4-pyridyl)benzene gives an open square grid coordination polymer in which the cavities were occupied by the dimers of MeOH and NO₃⁻.⁷ The reaction of 2,2'-bipyrazine and AgBF₄ can produce a distorted adamantine-shaped coordination polymer. When equimolar amounts of AgBF₄ and pyrazino[2,3-f]quinoxaline were mixed in MeNO₂, a three-dimensional coordination polymer was formed.⁸ There are also some polymers synthesized by flexible ligands, such as [Cd₂(NO₃)₄(Py₂C₃H₆(H₂O))_n], [Cd(NO₃)₂(Py₂C₄H₈(H₂O))_n], [Fe(NCS)₂(bpa)₂]_n [bpa = 1,2-bis(4-pyridyl)ethane], etc.⁹ Many reported coordination polymers concern transition metals; main group metallic coordination polymers are rare.

Recently, the third-order NLO properties of a series of coordination polymers such as [Co(NCS)₂(bpms)₂]_n, [Mn(SO₄)(4,4'-bpy)(H₂O)₂]_n, [Mn(N₃)₂(4,4'-bpy)]_n, [Mn(N₃)₂(bbp)₂]_n, {[Mn(NCS)₂(bbp)₂·0.25H₂O]_n (bbp = 4,4'-trimethylene-dipyridine), and [M(bbbt)₂(NCS)₂]_n (M = Co, Mn, or Cd; bbbt = 1,1'-(1,4-butanediyl)bis-1*H*-benzotriazole) have been reported.⁴ The results show that these coordination polymers have strong third-order NLO properties. In order to further synthesize novel coordination polymers and explore their third-order nonlinear optical (NLO) properties, especially d¹⁰ transition metals and main group metallic coordination polymers, we synthesized three flexible ligands 1,1'-(1,4-butanediyl)bis-1*H*-benzimidazole (bbbm), 1,1'-(1,4-butanediyl)bis-1*H*-benzotriazole (bbbt) and 1,1'-(1,3-propy-

lene)-bis-1*H*-benzotriazole (pbbt), and three coordination polymers [Pb(bbbm)₂(NO₃)₂]_n **1**, [Zn(bbbt)(NCS)₂]_n **2**, and [Zn(pbbt)(NCS)₂]_n **3**. Polymer **1** has a two-dimensional rhombohedral grid network structure and exhibits an interpenetrated layered packing mode. **2** possesses a novel one-dimensional concavo-convex chain, which is different from the reported linear chain, zigzag chain, helical chain, double-stranded chain, and ladder chain. **3** exhibits a one-dimensional zigzag chain structure. Their third-order nonlinear optical (NLO) properties were determined by the Z-scan technique. The third-order NLO susceptibility χ⁽³⁾ values of polymers **1**, **2**, and **3** were calculated to be 1.67 × 10⁻¹¹, 1.62 × 10⁻¹¹, and 1.08 × 10⁻¹¹ esu, respectively. We discuss the relationships between the crystal structures of coordination polymers and the observed NLO properties, and we deduce that the valence shell structures of metal ions may have some influence on the strength of NLO properties.

Experimental Section

General Information and Materials. All chemicals were of A. R. grade and used without further purification. UV-vis spectra were recorded, ranging from 250 to 800 nm, on a HP 8453 ultraviolet-visible spectrophotometer. IR spectra were performed on a PE spectrophotometer in the region of 400–4000 cm⁻¹. Carbon, hydrogen, and nitrogen analyses were carried out on a Carlo-Erba 1106 elemental analyzer. Proton NMR spectra were recorded on a Bruker DPX-400 spectrometer.

Synthesis of Ligands. Ligands 1,1'-(1,4-butanediyl)bis-1*H*-benzimidazole (bbbm), 1,1'-(1,4-butanediyl)bis-1*H*-benzotriazole (bbbt), and 1,1'-(1,3-propylene)bis-1*H*-benzotriazole (pbbt) were prepared according to the literature.¹⁰ Anal. Calcd for C₁₈H₁₈N₄ (bbbm) (%): C, 74.48; H, 6.25; N, 19.30. Found: C, 74.68; H, 6.38; N, 19.43. IR (KBr)/cm⁻¹: 3083m, 2924m, 1496s, 1462s, 1383s, 1332s, 751s. ¹H NMR (chloroform): δ 8.119 (2H), 7.816–7.839 (2H), 7.263–7.359 (6H), 4.225 (4H), 1.932–1.955 (4H).

Anal. Calcd for C₁₆H₁₆N₆ (bbbt) (%): C, 65.75; H, 5.48; N, 28.78. Found: C, 65.36; H, 5.44; N, 28.70. IR (KBr)/cm⁻¹: 3061m, 2951m, 1617w, 1569w, 1497w, 1455m, 1327s, 737s. ¹H NMR (Acetone): δ 7.842–7.866 (4H), 7.415–7.432 (4H), 4.835–4.868 (4H), 2.057–2.193 (4H).

Anal. Calcd for C₁₅H₁₄N₆ (pbbt) (%): C, 64.75; H, 5.04; N, 30.22. Found: C, 65.49; H, 5.02; N, 30.88. IR (KBr)/cm⁻¹: 3069m, 2960m, 1618w, 1564w, 1497w, 1459m, 1327s, 750s. ¹H NMR (chloroform): δ 7.833–7.871 (4H), 7.367–7.461 (4H), 4.876–4.909 (4H), 2.919–2.986 (2H).

Synthesis of [Pb(bbbm)₂(NO₃)₂]_n **1.** A methanol solution (5 mL) of bbbm (29 mg, 0.1 mmol) was dropwise added into an aqueous solution (2 mL) of Pb(NO₃)₂ (16.5 mg, 0.05 mmol) to give a clear solution. Colorless crystals (55% yield) suitable for X-ray diffraction were obtained 1 week later. Anal. Calcd for C₃₆H₃₆N₁₀O₆Pb (%): C, 47.41; H, 3.98; N, 15.36. Found: C, 47.01; H, 4.03; N, 15.14. IR (KBr)/cm⁻¹: 3104m, 2942m, 1500s, 1458s, 1385s, 1332s, 746s.

Synthesis of [Zn(bbbt)(NCS)₂]_n **2.** An aqueous solution (2 mL) of KSCN (19.4 mg, 0.2 mmol) was added into an aqueous solution (1 mL) of Zn(NO₃)₂·6H₂O (29.7 mg, 0.1 mmol), and then a methanol solution (5 mL) of bbbt (29.2 mg, 0.1 mmol) was slowly diffused into the above mixture. The resultant solution was left at room

- (3) (a) Halliday, D. A.; Burn, P. L.; Bradley, D. D. C.; Friend, R. H.; Gelsen, O. M.; Holmes, A. B.; Kraft, A.; Martens, J. H. F.; Pichler, K. *Adv. Mater.* **1993**, *5*, 40. (b) Bredas, J. L.; Adant, C.; Tackx, P.; Persoons, A.; Pierce, B. M. *Chem. Rev.* **1994**, *94*, 243. (c) Nakanishi, H. *Nonlinear Opt.* **1991**, *1*, 223. (d) Kobayashi, T. *IEICE Trans. Fundam.* **1992**, *E75-A*, 38. (e) Hou, H. W.; Ang, H. G.; Ang, S. G.; Fan, Y. T.; Low, M. K. M.; Ji, W.; Lee, Y. W. *Phys. Chem. Chem. Phys.* **1999**, *1*, 3145. (f) Zhang, C.; Y. Song, L.; Xu, Y.; Fun, H. K.; Fang, G. Y.; Wang, Y. X.; Xin, X. Q. *J. Chem. Soc., Dalton Trans.* **2000**, 2823. (g) Wang, Y.; Cheng, L. T. *J. Phys. Chem.* **1992**, *96*, 1530. (h) Shirk, J. S.; Lindle, J. R.; Bartoli, F. J.; Kafafi, Z. H.; Snow, A. W. In *Materials for Nonlinear Optics*; Marder, S. R., Sohn, J. E., Stucky, G. D., Eds.; American Chemical Society: Washington, 1992; p 626.
- (4) (a) Hou, H. W.; Song, Y. L.; Fan, Y. T.; Zhang, L. P.; Du, C. X.; Zhu, Y. *Inorg. Chim. Acta* **2001**, *316*, 140. (b) Hou, H. W.; Wei, Y. L.; Fan, Y. T.; Du, C. X.; Zhu, Y.; Song, Y. L.; Niu, Y. Y.; Xin, X. Q. *Inorg. Chim. Acta* **2001**, *319*, 212. (c) Evans, O. R.; Lin, W. B. *Chem. Mater.* **2001**, *13*, 3009. (d) Evans, O. R.; Lin, W. B. *Chem. Mater.* **2001**, *13*, 2705. (e) Lin, W. B.; Wang, Z. Y.; Ma, L. *J. Am. Chem. Soc.* **1999**, *121*, 11249. (f) Lin, W. B.; Evans, O. R.; Xiong, R. G.; Wang, Z. Y. *J. Am. Chem. Soc.* **1998**, *120*, 13272. (g) Hou, H. W.; Meng, X. R.; Song, Y. L.; Fan, Y. T.; Zhu, Y.; Lu, H. J.; Du, C. X.; Shao, W. H. *Inorg. Chem.* **2002**, *41*, 4068. (h) Hou, H. W.; Wei, Y. L.; Song, Y. L.; Zhu, Y.; Li, L. K.; Fan, Y. T. *J. Mater. Chem.* **2002**, *12*, 838.
- (5) (a) Ermer, O. *Adv. Mater.* **1991**, *3*, 608. (b) Inoue, K.; Hayamizu, T.; Iwamura, H.; Hashizume, D.; Ohashi, Y. *J. Am. Chem. Soc.* **1996**, *118*, 1803. (c) Kitazawa, T.; Nishikiori, S.; Kuroda, R.; Iwamoto, T. *J. Chem. Soc., Dalton Trans.* **1994**, 1029. (d) Fujita, M.; Kwon, Y. J.; Washizu, S.; Ogura, K. *J. Am. Chem. Soc.* **1994**, *116*, 1151.
- (6) David, M. L. G.; David, A. G.; David, J. W. *Angew. Chem., Int. Ed.* **1999**, *38*, 153.
- (7) Kumar, B.; Makoto, F. *J. Chem. Soc., Dalton Trans.* **2000**, 3805.
- (8) Alexander, J. B.; Neil, R. C.; Paul, A. C.; James, E. B. N.; Claire, W. *J. Chem. Soc., Dalton Trans.* **2000**, 3811.
- (9) (a) Plater, M. J.; Foreman, M. R. S. J.; Gelbrich, T.; Coles, S. J.; Hursthouse, M. B. *J. Chem. Soc., Dalton Trans.* **2000**, 3065. (b) Hernández, M. L.; Barandika, M. G.; Urriaga, M. K.; Cortés, R.; Lezama, L.; Arriortua, M. I.; Rojo, T. *J. Chem. Soc., Dalton Trans.* **1999**, 1401.

- (10) Xie, X. J.; Yang, G. S.; Cheng, L.; Wang, F. *Huaxue Shiji* **2000**, *22*, 222.

Table 1. Crystal Data and Structure Parameters of [Pb(bbbm)₂(NO₃)₂]_n **1**, [Zn(bbbt)(NCS)₂]_n **2**, and [Zn(pbtt)(NCS)₂]_n **3**

	1	2	3
empirical formula	C ₃₆ H ₃₆ N ₁₀ O ₆ Pb	C ₁₈ H ₁₆ N ₈ S ₂ Zn	C ₁₇ H ₁₄ N ₈ S ₂ Zn
fw	911.94	473.88	459.85
temp, K	291(2)	293(2)	291(2)
wavelength, Å	0.71073	0.71073	0.71073
cryst syst	monoclinic	triclinic	triclinic
space group	<i>c2/c</i>	<i>p1</i>	<i>p1</i>
unit cell dimens			
<i>a</i> , Å	20.731(4)	10.218(2)	8.7858(18)
<i>b</i> , Å	14.125(3)	13.251(3)	9.5635(19)
<i>c</i> , Å	15.886(3)	8.2097(16)	11.912(2)
α , deg	90	98.42(3)	85.60(3)
β , deg	128.71(3)	106.65(3)	86.93(3)
γ , deg	90	90.30(3)	81.38(3)
vol, Å ³	3630.2(13)	1052.2(4)	985.8(3)
<i>Z</i> ; calcd density, g/cm ³	4; 1.669	2; 1.496	2; 1.549
<i>F</i> (000)	1808	484	468
cryst size, mm	0.30 × 0.20 × 0.20	0.30 × 0.20 × 0.15	0.30 × 0.20 × 0.20
θ range for data collection, deg	1.91–27.52	1.56–27.61	1.72–27.49
index ranges	–26 ≤ <i>h</i> ≤ 13 –13 ≤ <i>k</i> ≤ 18 –16 ≤ <i>l</i> ≤ 20	0 ≤ <i>h</i> ≤ 13 –17 ≤ <i>k</i> ≤ 17 –10 ≤ <i>l</i> ≤ 9	–11 ≤ <i>h</i> ≤ 11 –12 ≤ <i>k</i> ≤ 0 –15 ≤ <i>l</i> ≤ 15
reflns collected/unique [<i>R</i> (int)]	6634/3745 [0.0295]	3033/3033 [0.0000]	3176/3176 [0.0000]
completeness to $2\theta = 27.52$, %	89.4	86.20	86.99
data/restraints/params	3745/0/257	3033/0/279	3176/0/270
GOF on <i>F</i> ²	1.067	1.055	1.078
final <i>R</i> indices [<i>I</i> > 2 σ (<i>I</i>)]			
<i>R</i> 1	0.0309	0.0647	0.0549
w <i>R</i> 2	0.0527	0.1464	0.1267
<i>R</i> indices (all data)			
<i>R</i> 1	0.0383	0.0888	0.0704
w <i>R</i> 2	0.0540	0.1587	0.1339
largest diff peak and hole, e Å ^{–3}	0.768 and –0.782	0.698 and –0.649	0.483 and –0.684

temperature. Colorless crystals suitable for X-ray diffraction were formed 1 month later (60% yield). Anal. Calcd for C₁₈H₁₆N₈S₂Zn (%): C, 45.58; H, 3.38; N, 23.63. Found: C, 45.12; H, 3.41; N, 23.26. IR (KBr)/cm^{–1}: 3094m, 2942m, 2076s, 1595w, 1493w, 1446m, 1338m, 752s.

Synthesis of [Zn(pbtt)(NCS)₂]_n **3.** A methanol solution (5 mL) of pbtt (27.8 mg, 0.1 mmol) was added into the mixture aqueous solution (4 mL) of Zn(NO₃)₂·6H₂O (29.7 mg, 0.1 mmol) and KSCN (19.4 mg, 0.2 mmol) to give a clear solution. Colorless crystals (55% yield) suitable for X-ray diffraction were obtained 3 weeks later. Anal. Calcd for C₁₇H₁₄N₈S₂Zn (%): C, 44.40; H, 3.07; N, 24.37. Found: C, 44.93; H, 3.01; N, 23.35. IR (KBr)/cm^{–1}: 3067m, 2943m, 2100s, 1592w, 1491w, 1462m, 1329m, 757s.

Crystal Structure Determination. A colorless single crystal suitable for X-ray determination was mounted on a glass fiber. All data were collected at room temperature on a Rigaku RAXIS-IV image plate area detector with graphite-monochromated Mo K α radiation ($\lambda = 0.71073$ Å). The structures were solved by direct methods and expanded using Fourier techniques. The non-hydrogen atoms were refined anisotropically. Hydrogen atoms were included but not refined. The final cycle of full-matrix least-squares refinement was based on observed reflections and variable parameters. All calculations were performed using the SHELXL-97 crystallographic software package.¹¹ Table 1 shows crystallographic crystal data and processing parameters of polymers **1**, **2**, and **3**. Selected bond lengths and bond angles are listed in Table 2.

CCDC reference numbers are 185304, 185305, and 190834.

See <http://www.ccdc.cam.ac.uk> for crystallographic data in CIF.

Molecular Weight Measurements. The molecular weight and molecular weight distribution of the polymers were determined at 40 °C with gel permeation chromatography (Waters Associates

Table 2. Selected Bond Lengths (Å) and Bond Angles (deg) of Polymers [Pb(bbbm)₂(NO₃)₂]_n **1**, [Zn(bbbt)(NCS)₂]_n **2**, and [Zn(pbtt)(NCS)₂]_n **3**

[Pb(bbbm) ₂ (NO ₃) ₂] _n 1 ^a			
Pb(1)–N(1)#1	2.588(3)	Pb(1)–O(1)#1	2.628(4)
Pb(1)–N(1)	2.588(3)	Pb(1)–N(3)#1	2.788(3)
Pb(1)–O(1)	2.628(4)	Pb(1)–N(3)	2.788(3)
N(1)#1–Pb(1)–N(1)	72.95(12)	O(1)–Pb(1)–N(3)#1	98.96(13)
N(1)#1–Pb(1)–O(1)	75.80(11)	O(1)#1–Pb(1)–N(3)#1	87.14(14)
N(1)–Pb(1)–O(1)	88.53(11)	N(1)#1–Pb(1)–N(3)	142.35(9)
N(1)#1–Pb(1)–O(1)#1	88.53(11)	N(1)–Pb(1)–N(3)	73.32(9)
N(1)–Pb(1)–O(1)#1	75.80(11)	O(1)–Pb(1)–N(3)	87.14(14)
O(1)–Pb(1)–O(1)#1	160.60(15)	O(1)#1–Pb(1)–N(3)	98.96(13)
N(1)#1–Pb(1)–N(3)#1	73.32(9)	N(3)#1–Pb(1)–N(3)	143.42(13)
N(1)–Pb(1)–N(3)#1	142.35(9)		
[Zn(bbbt)(NCS) ₂] _n 2 ^b			
Zn(1)–N(8)	1.925(6)	Zn(1)–N(1)	2.011(5)
Zn(1)–N(7)	1.941(5)	Zn(1)–N(4)	2.039(5)
N(8)–Zn(1)–N(7)	122.6(2)	N(8)–Zn(1)–N(4)	105.3(2)
N(8)–Zn(1)–N(1)	108.4(2)	N(7)–Zn(1)–N(4)	103.4(2)
N(7)–Zn(1)–N(1)	105.5(2)	N(1)–Zn(1)–N(4)	111.4(2)
[Zn(pbtt)(NCS) ₂] _n 3 ^c			
Zn(1)–N(8)	1.920(3)	Zn(1)–N(1)	2.018(3)
Zn(1)–N(7)	1.955(3)	Zn(1)–N(4)	2.056(3)
N(8)–Zn(1)–N(7)	115.36(14)	N(8)–Zn(1)–N(4)	107.97(12)
N(8)–Zn(1)–N(1)	115.38(12)	N(7)–Zn(1)–N(4)	101.03(12)
N(7)–Zn(1)–N(1)	102.06(12)	N(1)–Zn(1)–N(4)	114.25(10)

^a Symmetry transformations used to generate equivalent atoms in polymer **1**: #1 $-x + 1, y, -z + 3/2$; #2 $-x + 1/2, y - 1/2, -z + 1/2$; #3 $-x + 1/2, y + 1/2, -z + 1/2$. ^b Symmetry transformations used to generate equivalent atoms in polymer **2**: #1 $-x + 1, -y + 2, -z + 2$; #2 $-x + 1, -y + 1, -z + 1$. ^c Symmetry transformations used to generate equivalent atoms in polymer **3**: #1 $x, y - 1, z$; #2 $x, y + 1, z$.

model HPLC/GPC 515 liquid chromatography, equipped with a refractive index detector and μ -Styragel columns and calibrated with

(11) Sheldrick, G. M. *SHELXTL-97 Program for Refining Crystal Structure Refinement*; University of Göttingen: Göttingen, Germany, 1997.

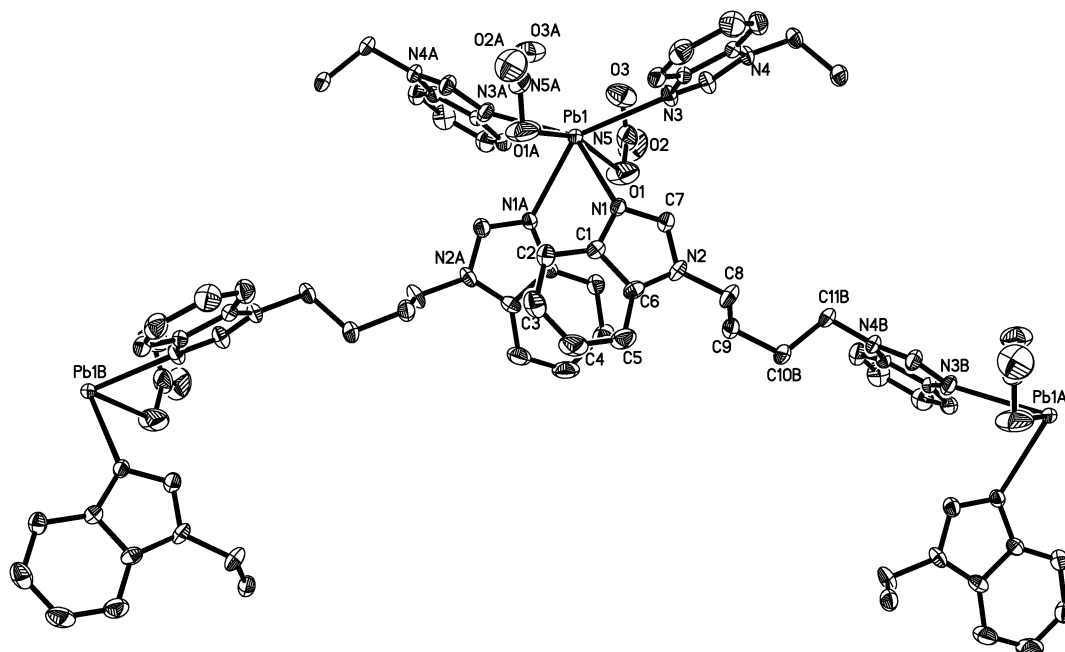


Figure 1. Structural unit of $[\text{Pb}(\text{bbb}\text{m})_2(\text{NO}_3)_2]_n$, with atom numberings, showing 30% thermal ellipsoids. Hydrogen atoms have been omitted for clarity.

standard polystyrene), using DMF as eluent and a flow rate of 1.0 mL min^{-1} .

Nonlinear Optical Measurements. A DMF solution of polymer **1**, **2**, or **3** was placed in a 1-mm quartz cuvette for NLO measurements. Their nonlinear refraction and nonlinear absorption were measured with a linearly polarized laser light ($\lambda = 532$ nm; pulse widths = 7 ns) generated from a Q-switched and frequency-doubled Nd:YAG laser. The spatial profiles of the optical pulses were nearly Gaussian. The laser beam was focused with a 25-cm focal-length focusing mirror. The radius of the beam waist was measured to be 35 ± 5 μm (half-width at $1/e^2$ maximum). The interval between the laser pulses was chosen to be ~ 5 s for operational convenience. The incident and transmitted pulse energies were measured simultaneously by two Laser Precision detectors (RjP-735 energy probes), which were linked to a computer by an IEEE interface. The NLO properties of the samples were manifested by moving the samples along the axis of the incident beam (Z -direction) with respect to the focal point.¹² An aperture of 0.5 mm in radius was placed in front of the detector to assist the measurement of the self-focusing effect.

Results and Discussion

Description of Crystal Structures. The structural unit of polymer **1** is shown in Figure 1. The Pb(II) ion coordinates to four nitrogen donors from different bbbm ligands and two oxygen atoms from two nitrate anions to form a distorted octahedral environment, and lies on a crystallographic 2-fold axis. The N1–Pb1–N3A and N1A–Pb1–N3 bond angles are only $142.35(9)^\circ$, and the N1–Pb1–N1A and N3–Pb1–N3A bond angles are $72.95(12)^\circ$ and $143.42(13)^\circ$, respectively, so there is a significant departure from ideal planarity of the PbN_4 unit (the mean deviation from plane is 0.2153 Å). Pb1–N1 and Pb1–N1A bond lengths (2.588(3) Å) are shorter than the Pb1–N3 and Pb1–N3A bond lengths

(2.788(3) Å). In the complex $[\text{PbL}(\text{ClO}_4)]\text{ClO}_4$ (L = 1,4,7-tris(pyrazol-1-ylmethyl)-1,4,7-triazacyclononane), the Pb–N (from pyrazole) bond lengths range from 2.539(10) to 2.860(10) Å.¹³

Nitrate anion, as a monodentate ligand, coordinates to the Pb(II). All the O–N–O bond angles (O1–N5–O3, $118.8(4)^\circ$; O1–N5–O2, $119.0(5)^\circ$; O3–N5–O2, $121.9(5)^\circ$) and N–O bond lengths (N5–O1, 1.238(5) Å; N5–O2, 1.240(5) Å; N5–O3, 1.239(5) Å) correspond to those found in many simple ionic nitrate salts. The O1–Pb1–O1A bond angle is $160.60(15)^\circ$. The Pb1–O1 bond length of 2.628(4) Å is rather shorter than Pb–O distances in lead nitrate (2.805 Å)¹⁴ and the compound $[\text{Pb}(\text{L})][\text{NO}_3]_2$ (2.74(3)–3.17(4) Å) (L = 1,5,9,13-tetraazacyclohexadecane),¹⁵ quite similar to the sum of the ionic radius of Pb(II) and the van der Waals radius of oxygen (2.67 Å).¹⁶ Therefore, we presume that the interactions between Pb1 and O1 are covalent rather than electrostatic.

In Figure 2, the polymer consists of two-dimensional rhombohedral grid networks. The two-dimensional sheets are parallel to the crystallographic bc plane and stack with an interpenetrating mode. The distance between two adjacent layers is 10.359 Å. Each rhombohedral grid is formed by four bbbm ligands and four Pb(II) ions to give a 44-membered metallocyclic ring, the angle between two ligands is 120.7° or 59.3° , the diagonal-to-diagonal distances are 24.809×14.125 Å, and the dimensions of the grid are 14.274×14.274 Å. The dihedral angle between two benzimidazole planes from the same bbbm is 69.6° . The dihedral

(12) Sheik-Bahae, M.; Said, A. A.; Van Stryland, E. W. *Opt. Lett.* **1989**, *14*, 955.

(13) Massimo, D. V.; Matteo, G.; Fabrizio, M.; Piero, S. *J. Chem. Soc., Dalton Trans.* **1996**, 1173.

(14) Hamilton, W. C. *Acta Crystallogr.* **1957**, *10*, 103.

(15) Nathaniel, W. A.; Eirian, H. C.; Peter, M. *J. Chem. Soc., Dalton Trans.* **1984**, 2813.

(16) Wiegardt, K.; Kleine-Boymann, M.; Nuber, B.; Weiss, J.; Zsolnai, L.; Huttner, G. *Inorg. Chem.* **1986**, *25*, 1647.

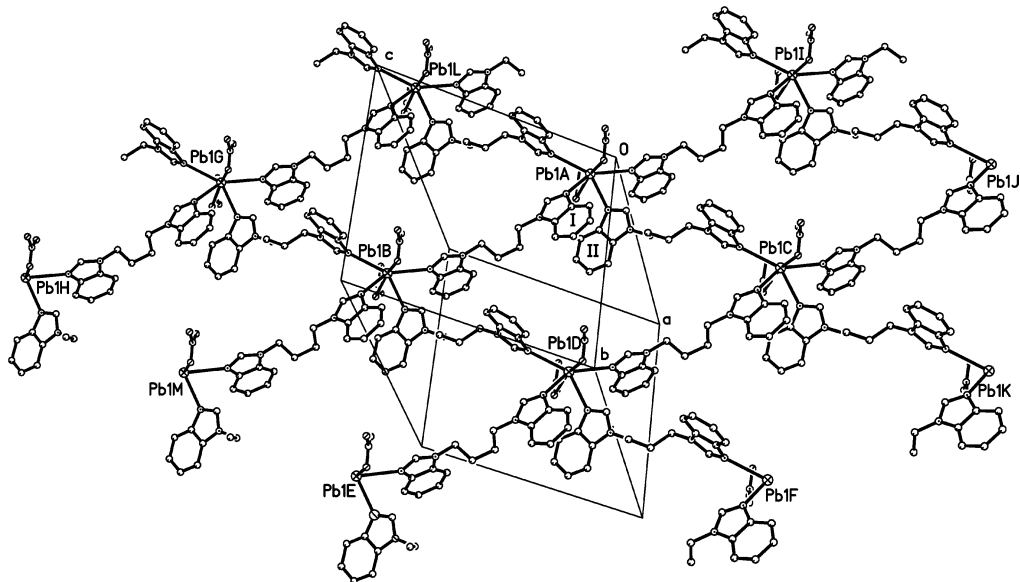


Figure 2. The two-dimensional rhombohedral grid structure of $[\text{Pb}(\text{bbb}\text{m})_2(\text{NO}_3)_2]_n$.

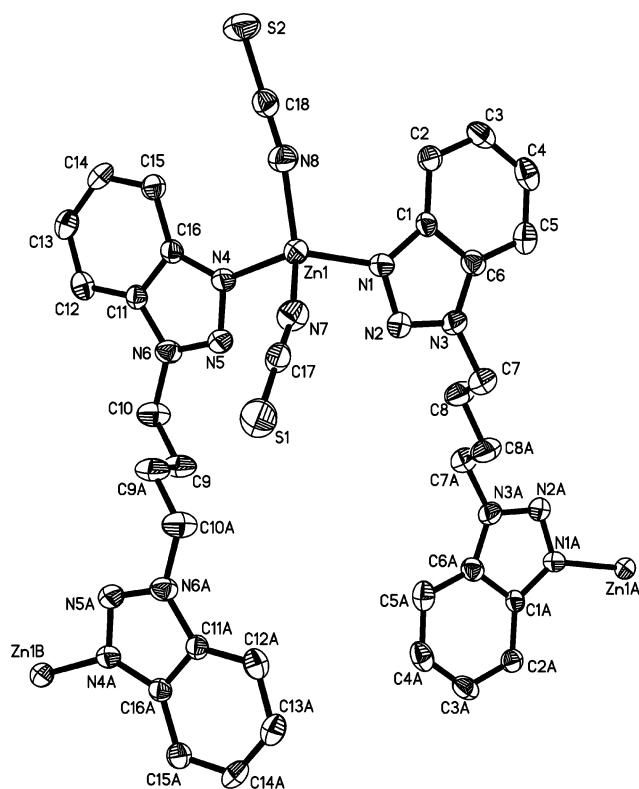


Figure 3. Structural unit of $[\text{Zn}(\text{bbbt})(\text{NCS})_2]_n$ with atom numberings, showing 30% thermal ellipsoids. Hydrogen atoms have been omitted for clarity.

angle between planes I and II (Figure 2) is 23° , and the shortest distances between the two planes is 3.2115 \AA , so there are π - π interactions between benzimidazole units. In addition, there are two monodentate nitrate ions that lie up and down the rhombohedral grid plane.

The crystal structure of polymer **2** is depicted in Figure 3. The coordination geometry of each Zn(II) ion is a slightly distorted tetrahedron, in which each Zn(II) ion is coordinated by two nitrogen atoms from bbbt ligands and two nitrogen atoms from isothiocyanate (NCS^-) groups, the angles around

Zn(II) ions are from $103.4(2)$ – $122.6(2)^\circ$, and Zn– N_{bbbt} bond lengths ($2.011(5)$, $2.039(5) \text{ \AA}$) are longer than those of Zn– N_{NCS} ($1.925(6)$, $1.941(5) \text{ \AA}$). Zn–N bond lengths correspond to those observed in $[\text{Zn}(\text{tp})(4,4'\text{-bipyridine})]$ (av 2.170 \AA) (tp = terephthalate) and $[\text{Zn}(4,4'\text{-bpy})(\text{H}_2\text{O})_3(\text{ClO}_4)]$ (ClO_4)· $(4,4'\text{-bpy})_{1.5}\cdot\text{H}_2\text{O}$ (av 2.110 \AA).¹⁷

Every zinc ion is linked by two *trans*-bbbt with torsion angles of 177.8° for $\text{N3}-\text{C7}-\text{C8}-\text{C8A}$ and -177.8° for $\text{N3A}-\text{C7A}-\text{C8A}-\text{C8}$, and each *trans*-bbbt bridges two zinc ions together via nitrogen atoms to form a one-dimensional concavo-convex chain; the Zn–Zn distance is 13.139 \AA (Figure 4). Table 3 summarizes five structural types of the reported one-dimensional polymers. For example, $[\text{Cu}(4,4'\text{-bpy})(\text{BF}_4)_2(\text{H}_2\text{O})_2]\cdot(4,4'\text{-bpy})$ is a one-dimensional linear polymer, $[\text{HgI}_2(\text{bpmp})]_n$ [bpmp = *N,N'*-bis(4-pyridylmethyl)-piperazine] possesses a zigzag chain structure, and $[\text{Cu}(\text{pyz})_2(\text{CF}_3\text{SO}_3)]_n$ (pyz = pyrazine), $[\text{Co}(\text{Py}_2\text{S})_2(\text{NCS})_2\cdot 2\text{H}_2\text{O}]_n$, and $[\text{Co}(4,4'\text{-bpy})_{1.5}(\text{NO}_3)_2]_n$ give helical chain structure, double-stranded chain structure, and ladder chain structure, respectively. Polymer **2**'s concavo-convex chain structure is different from those of the reported polymers. It is a new type of one-dimensional polymer.

Furthermore, there are stable π - π interactions among benzene rings of adjacent chains; these benzene rings are parallel with an interplanar distance of 3.516 \AA .

Figure 5 gives the crystal structural unit of polymer **3**. The angles around Zn(II) ions are close to $109^\circ 28'$ ($101.03(12)^\circ$, $102.06(12)^\circ$, $107.97(12)^\circ$, $114.25(10)^\circ$, $115.36(14)^\circ$, $115.38(12)^\circ$), and Zn– N_{pbtt} bond lengths ($2.018(3)$, $2.056(3) \text{ \AA}$) are longer than those of Zn– N_{NCS} ($1.920(3) \text{ \AA}$, $1.955(3) \text{ \AA}$), so central Zn ion is located in a slightly distorted tetrahedron environment. All of the bond lengths are very close to those observed in polymer **2**. Each Zn(II) ion is coordinated by two nitrogen atoms from *trans*-pbtt ligands and two nitrogen atoms from isothiocyanate (NCS^-) groups.

(17) (a) Tao, J.; Tong, M. L.; Chen, X. M. *J. Chem. Soc., Dalton Trans.* **2000**, 3699. (b) Tong, M. L.; Cai, J. W.; Yu, X. L.; Chen, X. M.; Ng, S. W.; Mak, T. C. W. *Aust. J. Chem.* **1998**, *51*, 637.

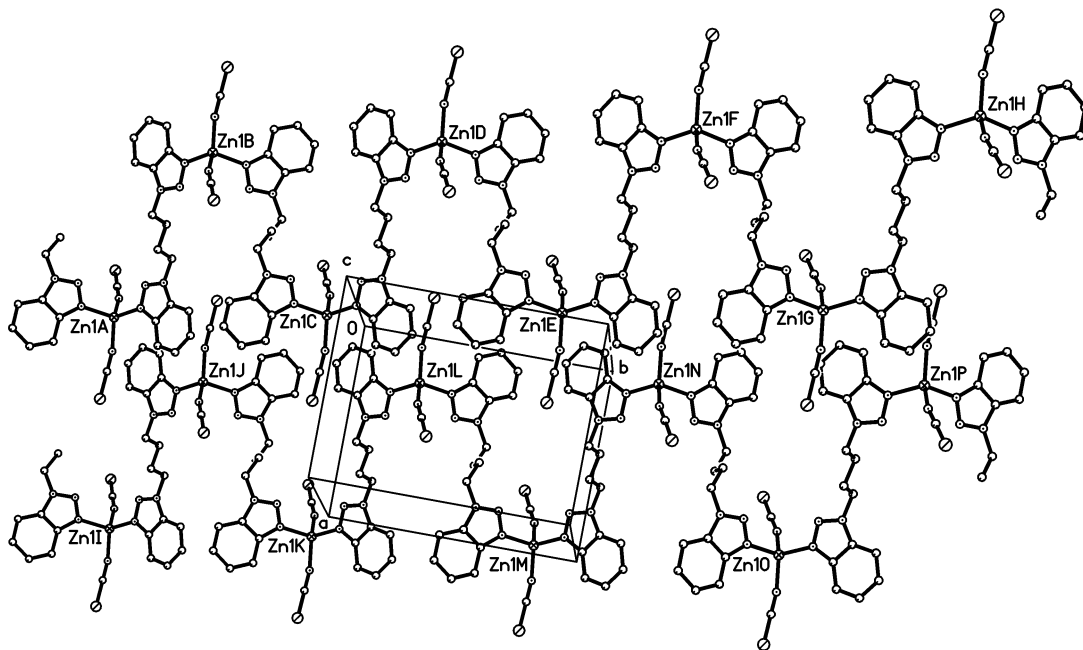


Figure 4. The crystal structure of $[\text{Zn}(\text{bbtt})(\text{NCS})_2]_n$.

Table 3. Structural Types of Reported One-Dimensional Polymers

chain types	examples	refs	
linear	$[\text{Cu}(4,4'\text{-bpy})(\text{BF}_4)_2(\text{H}_2\text{O})_2] \cdot (4,4'\text{-bpy})$	23	
	$[\text{Mn}(\mu\text{-}4,4'\text{-bipy})(4,4'\text{-bipy})(\text{NCS})_2(\text{HO})_2]_n$	24	
	$[\text{Cu}(\gamma\text{-bpy})(\text{H}_2\text{O})_2(\text{ClO}_4)_2] \cdot (\gamma\text{-bpy})_n$	25	
	$[\text{Zn}(\text{H}_2\text{O})_4(\text{bipy})][\text{NO}_3]_2 \cdot \text{bipy}$	26	
	$[\text{Zn}(\text{H}_2\text{O})_4(\text{bipy})](\text{NO}_3)_2 \cdot 2\text{bipy} \cdot 3\text{H}_2\text{O}$	26	
	$[\text{Zn}(\text{H}_2\text{O})_4(\text{bipy})][\text{O}_3\text{SCF}_3]_2 \cdot 2\text{bipy}$	26	
	$[\text{Fe}(4,4'\text{-bpy})(\text{H}_2\text{O})_3(\text{ClO}_4)](\text{ClO}_4) \cdot 1.5(4,4'\text{-bpy}) \cdot \text{H}_2\text{O}$	26	
	zigzag	$[\text{Cu}(4,4'\text{-bpy})(\text{MeCN})_2](\text{BF}_4)$	27
$[\text{Cu}(\text{dmp})(4,4'\text{-bpy})](\text{BF}_4) \cdot \text{MeCN}$ (dmp = 2,9-dimethyl-1,10-phenanthroline)		28	
$[\text{HgI}_2(\text{bpmp})]_n$ [bpmp = N,N' -bis(4-pyridylmethyl)piperazine]		29	
$[\text{Zn}(\text{pbtt})(\text{NCS})_2]_n$		<i>a</i>	
helical	$[\text{AgL}(\text{NO}_3)]_n$	30	
	{L = (4 <i>R</i> ,5 <i>R</i>)- <i>trans</i> -4,5-bis[(diphenyl-phosphino)methyl]-2,2-dimethyl-1,3-dioxalane}		
	$\{[\text{AgL}]\text{NO}_3 \cdot 2\text{HO}\}_n$	31	
	{L = (1 <i>R</i> ,2 <i>R</i>)-cyclohexane-1,2-diamine}		
	$\{[\text{Cu}(\text{MeCN})\text{L}]\text{BF}_4 \cdot 0.5\text{CH}_2\text{Cl}_2\}_n$	32	
	(L = 2,2'-bi-naphthyridine)		
	$[\text{Cu}(\text{pyz})_2(\text{CF}_3\text{SO}_3)]_n$ (pyz = pyrazine)	33	
	$[\text{Cu}(2,5\text{-Me}_2\text{pyz})_2(\text{CF}_3\text{SO}_3)]_n$	34	
	(Me ₂ pyz = dimethylpyrazine)		
	$[\text{Co}(\text{Py}_2\text{S})_2(\text{NCS})_2 \cdot 2\text{H}_2\text{O}]_n$	35	
double-stranded	$[\text{Fe}(\text{NCS})_2(\text{bpa})_2]_n$	9b	
	[bpa = 1,2-bis(4-pyridyl)-ethane]		
	ladder	$[\text{Ni}(4,4'\text{-bpy})_{2.5}(\text{H}_2\text{O})_2(\text{ClO}_4)_2] \cdot 1.5(4,4'\text{-bpy}) \cdot 2\text{H}_2\text{O}]_n$	36
		$[\text{Co}(4,4'\text{-bpy})_{1.5}(\text{NO}_3)_2]_n$	37
	$\{[\text{Cu}_2\text{L}_3(\text{MeCN})_2](\text{PF}_6)_2\}_n$	38	
	{L = 1,4-bis(4-pyridyl)butadiyne}		
	$[\text{Cd}(\text{dpb})_3(\text{NO}_3)_2]_n$	39	
	(dpb = $\text{PyCH}_2\text{C}_6\text{H}_4\text{CH}_2\text{Py}$)		
$[\text{Co}(4,4'\text{-bipy})(\text{CH}_3\text{COO})_2]_n$	40		
$[\text{Zn}(\text{bpethy})_3(\text{NO}_3)_4]_n$	41		
[bpethy = 1,2-bis-(4-pyridyl)ethyne]			
concavo-convex	$[\text{Zn}(\text{bbtt})(\text{NCS})_2]_n$	<i>a</i>	

^a This work.

In each *trans*-pbtt ligand the dihedral angle of the two benzotriazole planes is 135.4°. Every zinc ion is linked by two *trans*-pbtt ligands with torsion angles of 79.3° for

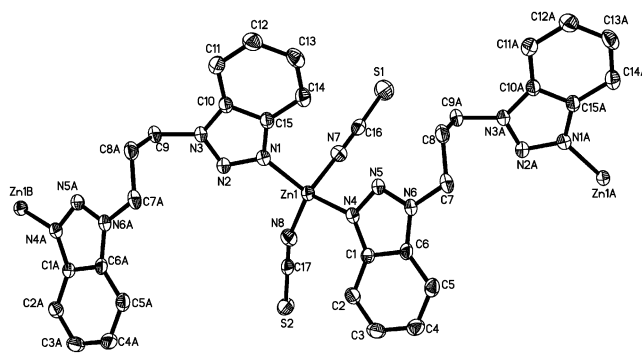


Figure 5. Structural unit of $[\text{Zn}(\text{pbtt})(\text{NCS})_2]_n$ with atom numberings, showing 30% thermal ellipsoids. Hydrogen atoms have been omitted for clarity.

$\text{N6A}-\text{C7A}-\text{C8A}-\text{C9}$ and -74.0° for $\text{N3}-\text{C9}-\text{C8A}-\text{C7A}$, and each *trans*-pbtt bridges two zinc ions together via nitrogen atoms to form a one-dimensional zigzag chain; the Zn–Zn distance (9.564 Å) is shorter than that of polymer **2** (13.139 Å). These zigzag chains are arranged as a ...ABAB... layered structure (Figure 6). In the same layer, two chains are connected by the weak interactions between Zn(II) ions and S1 (the $\text{Zn} \cdots \text{S2}$ distance is 3.95 Å; the normal Zn–S coordination bond length is 2.261–2.327 Å¹⁸), and $\pi-\pi$ interactions between benzene rings (such as benzene rings I and II) which are parallel to each other and have an interplanar distance of av 3.543 Å. Moreover, between adjacent layers, there are also two kinds of interactions. One is the weak $\text{C}-\text{H} \cdots \text{S1}$ hydrogen bond; the distances between the S1 atom and H atoms from benzene rings are 2.918 and 2.847 Å, respectively, close to those of the reported polymer $[\text{Fe}(\text{NCS})(\text{bpa})_2]$ [the S–H distance is 2.79 Å; bpa = 1,2-bis(4-pyridyl)ethane];⁹ the other is the π -stacking interaction between benzene rings (such as benzene rings III and IV),

(18) Spencer, D. J.; Blake, A. J.; Parsons, S.; Schröder, M. *J. Chem. Soc., Dalton Trans.* **1999**, 1041.

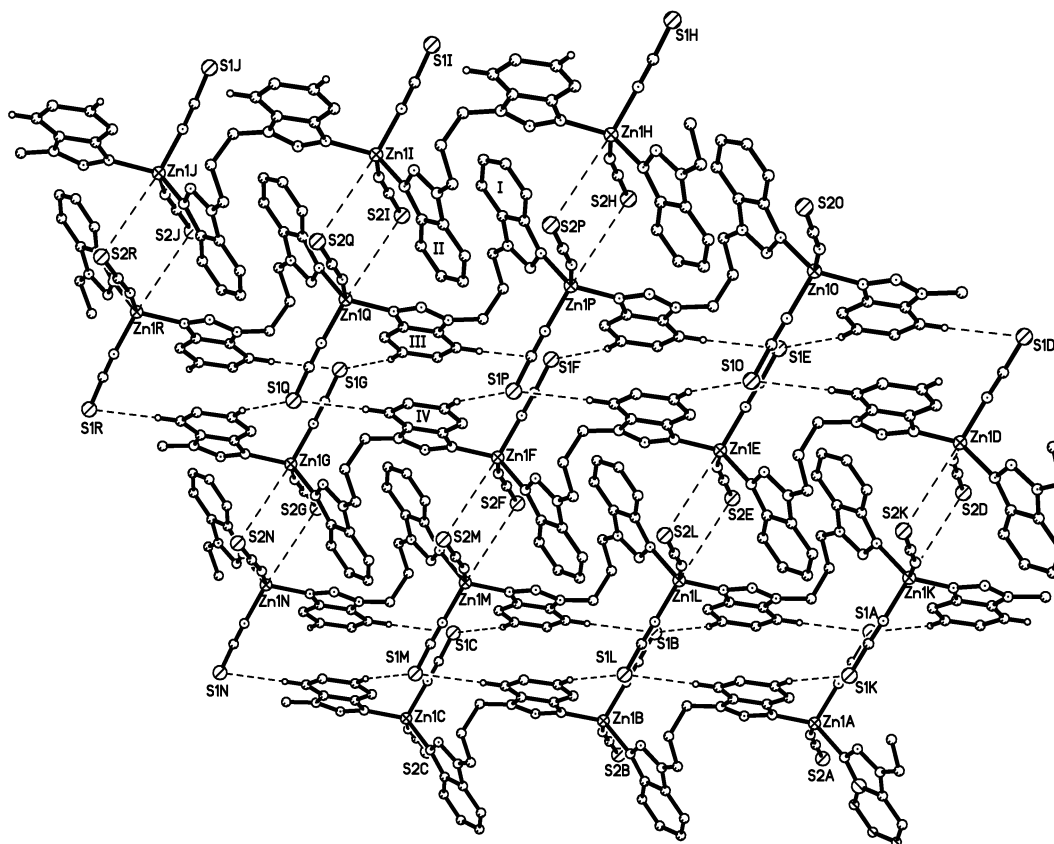


Figure 6. The layered structure of $[\text{Zn}(\text{pbtt})(\text{NCS})_2]_n$.

which are arranged in face-to-face fashion with interplanar distances of $\text{av } 3.553 \text{ \AA}$.

Although the $\pi-\pi$ interactions in each layer and between layers are weak compared to the metal–nitrogen coordinating bonds, these kinds of interactions were important in the molecular assembly.

Polymers **2** and **3** have similar molecular formulas, but their structures show a great difference due to the little difference between bbbt and pbtt. So the structures of coordination polymers can be altered by slight changes of the ligands.

Nonlinear Optical Properties. The UV–visible spectra of polymers **1**, **2**, and **3** in DMF solution show that there is only one absorption peak at 271 nm for **1**, 274 nm for **2**, and 278 nm for **3**. The absorptive bands could be attributed to the $\pi-\pi^*$ transitions of the ligands. All three polymers give very low linear absorption ranging from 300 to 800 nm, which is similar to the behavior of other coordination polymers.⁴ We determined the molecular weights of polymers **1**, **2**, and **3** in DMF solution. The results show that the number average molecular weights (M_n) are 3148 for polymer **1**, 4805 for polymer **2**, and 7218 for polymer **3**. The weight average molecular weights (M_w) are 4159, 7105, and 9354 for polymers **1**, **2**, and **3**, respectively. Thus we confirm that polymers **1**, **2**, and **3** are intact in DMF solution.

The NLO properties of polymers **1**, **2**, and **3** were measured in DMF solution of $3.4 \times 10^{-4} \text{ mol dm}^{-3}$ for polymer **1**, $5.2 \times 10^{-4} \text{ mol dm}^{-3}$ for polymer **2**, and $4.35 \times 10^{-4} \text{ mol dm}^{-3}$ for polymer **3**. Polymer **1** exhibits very strong

third-order NLO absorptive and refractive properties, and polymers **2** and **3** possess weaker NLO absorptive and strong NLO refractive properties. The NLO absorption components were evaluated by Z-scan experiment under an open aperture configuration. The NLO refractive properties were assessed by dividing the normalized Z-scan data obtained under the closed aperture configuration by the normalized Z-scan data obtained under the open aperture configuration. Equations 1–3 describe the third-order NLO process:¹⁹

$$T(Z) = \frac{1}{\sqrt{\pi}q(Z)} \int_{-\infty}^{+\infty} \text{Im}[1 + q(Z)]e^{-\tau^2} d\tau \quad (1)$$

$$q(Z) = \alpha_2 I_i(Z) \frac{1 - e^{-\alpha_0 L}}{\alpha_0} \quad (2)$$

$$n_2 = \frac{\lambda \alpha_0}{0.812\pi I(1 - e^{-\alpha_0 L})} \Delta T_{V-P} \quad (3)$$

where Z is the distance of the sample from the focal point; α_0 and α_2 are the linear and nonlinear absorption coefficients, respectively; $I_i(Z)$ is the peak irradiation intensity; L is the sample thickness; λ is the wavelength of the laser; n_2 is nonlinear refractive indexes of the sample; and ΔT_{V-P} is the difference between the normalized transmittance values at valley and peak portions.

(19) (a) Sheik-Bahae, M.; Said, A. A.; Stryland, E. W. V. *Opt. Lett.* **1989**, *14*, 955. (b) Sheik-Bahae, M.; Said, A. A.; Wei, T. H.; Hagan, D. J.; Stryland, E. W. V. *IEEE J. Quantum Electron.* **1990**, *26*, 760.

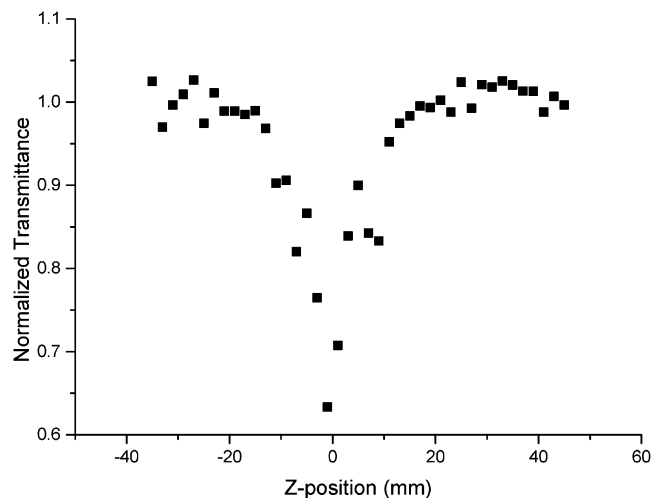


Figure 7. The NLO absorption data of $[\text{Pb}(\text{bbb}\text{m})_2(\text{NO}_3)_2]_n$ in a $3.4 \times 10^{-4} \text{ mol dm}^{-3}$ DMF solution at 532 nm with incident energy of $150 \mu\text{J}$. The data were collected under an open aperture configuration.

Figure 7 depicts NLO absorptive properties of polymer **1**. The figure clearly illustrates that the absorption increases as the incident light irradiance rises. It can be seen from Figure 7 that the normalized transmittance drops to about 61% at the focus, which shows that polymer **1** has a strong NLO absorptive effect. The third-order NLO absorptive coefficient α_2 was calculated to be $5.8 \times 10^{-9} \text{ m W}^{-1}$. Most of the reported materials with good third-order NLO absorptions are cluster compounds and coordination polymers, such as $[\text{W}_2\text{Ag}_4\text{S}_8(\text{AsPh}_3)_4]$ ($\alpha_2 = 2.8 \times 10^{-9} \text{ m W}^{-1}$),²⁰ $\{[\text{Et}_4\text{N}]_2[\text{MoS}_4\text{Cu}_4(\text{CN})_4]\}_n$ ($\alpha_2 = 1.5 \times 10^{-9} \text{ m W}^{-1}$), $\{[\text{Et}_4\text{N}]_2[\text{WS}_4\text{Cu}_4(\text{CN})_4]\}_n$ ($\alpha_2 = 1.6 \times 10^{-9} \text{ m W}^{-1}$),³ $[\text{Co}(\text{bbbt})_2(\text{NCS})_2]_n$ ($\alpha_2 = 5.4 \times 10^{-9} \text{ m W}^{-1}$), $[\text{Mn}(\text{bbbt})_2(\text{NCS})_2]_n$ ($\alpha_2 = 5.2 \times 10^{-9} \text{ m W}^{-1}$), and $[\text{Cd}(\text{bbbt})_2(\text{NCS})_2]_n$ ($\alpha_2 = 5.0 \times 10^{-9} \text{ m W}^{-1}$).⁴ It is obvious that polymer **1** exhibits stronger NLO absorption, and its α_2 value is larger than those of the reported cluster compounds and coordination polymers. Polymers **2** and **3** exhibit weaker third-order NLO absorptive effects. Polymers **1**, **2**, and **3** have similar ligands, but they show different third-order NLO absorptive properties. The third-order NLO properties of coordination polymers can be altered through metal atom manipulation.

Panels a–c in Figure 8 depict the NLO refractive properties of polymers **1**, **2**, and **3**, respectively. The data show that polymers **1**, **2**, and **3** have a similar positive sign for the refractive nonlinearity; the valley/peak pattern of the normalized transmittance curve shows characteristic self-focusing behavior.

It can be seen from Figure 8a that the difference of valley–peak positions, $\Delta Z_{\text{V-P}}$, is 18 mm; the difference between normalized transmittance values at valley and peak portions, $\Delta T_{\text{V-P}}$, is 0.32. The refractive index n_2 of polymer **1** is calculated to be $4.67 \times 10^{-18} \text{ m}^2 \text{ W}^{-1}$ by eq 3. For polymer **2**, $\Delta Z_{\text{V-P}}$ and $\Delta T_{\text{V-P}}$ are 12 mm and 0.31, respectively (Figure 8b); the n_2 value is $4.53 \times 10^{-18} \text{ m}^2 \text{ W}^{-1}$. In Figure 8c, $\Delta Z_{\text{V-P}}$ is 8 mm and $\Delta T_{\text{V-P}}$ is 0.10; the n_2 value of

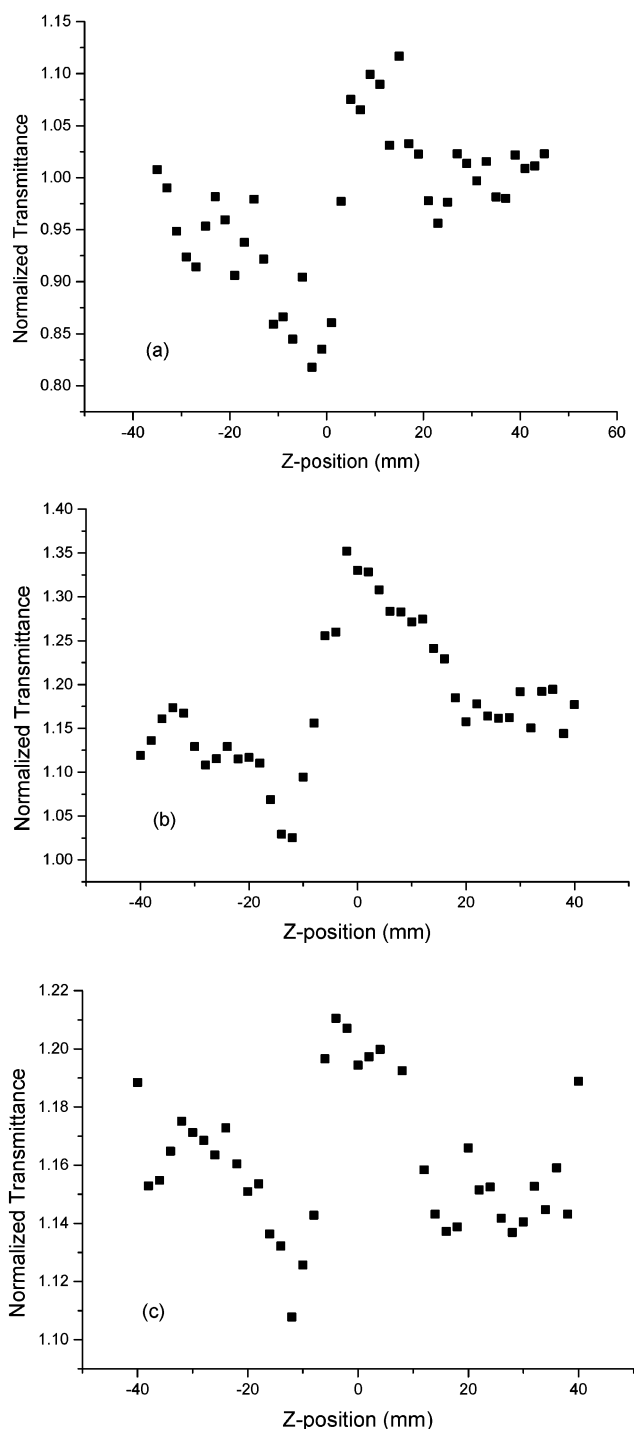


Figure 8. The data were assessed by dividing the normalized Z-scan data obtained under the closed aperture configuration by the normalized Z-scan data obtained under the open aperture configuration. (a) The self-focusing effects of $[\text{Pb}(\text{bbb}\text{m})_2(\text{NO}_3)_2]_n$ in a $3.4 \times 10^{-4} \text{ mol dm}^{-3}$ DMF solution at 532 nm with incident energy of $150 \mu\text{J}$. (b) The self-focusing effects of $[\text{Zn}(\text{bbtt})(\text{NCS})_2]_n$ in a $5.2 \times 10^{-4} \text{ mol dm}^{-3}$ DMF solution at 532 nm with incident energy of $150 \mu\text{J}$. (c) The self-focusing effects of $[\text{Zn}(\text{pbtt})(\text{NCS})_2]_n$ in a $4.35 \times 10^{-4} \text{ mol dm}^{-3}$ DMF solution at 532 nm with incident energy of $150 \mu\text{J}$.

polymer **3** is $3.02 \times 10^{-18} \text{ m}^2 \text{ W}^{-1}$. Nonlinear refractive indexes n_2 were reported for some best performing NLO materials such as inorganic oxides like SiO_2 ($n_2 = 2 \times 10^{-20} \text{ m}^2 \text{ W}^{-1}$) and RN ($n_2 = 1.3 \times 10^{-18} \text{ m}^2 \text{ W}^{-1}$), semiconductors like CdS ($n_2 = 2.5 \times 10^{-18} \text{ m}^2 \text{ W}^{-1}$), CdSe ($n_2 = -7.3 \times$

(20) Sakane, G.; Shibahare, T.; Hou, H. W.; Xin, X. Q.; Shi, S. *Inorg. Chem.* **1995**, *34*, 4785.

Table 4. The $\chi^{(3)}$ Value of Some Reported NLO Materials^a

compounds	$\chi^{(3)}/\text{esu}$	λ (nm)	ref
{[Et ₄ N] ₂ [MoS ₄ Cu ₄ (CN) ₄]} _n	4.58×10^{-9}	532	3f
{[Et ₄ N] ₂ [WS ₄ Cu ₄ (CN) ₄]} _n	5.12×10^{-9}	532	3f
[Et ₄ N] ₃ [WOS ₃ (CuBr) ₃ (μ_2 -Br)]·2H ₂ O	2.6×10^{-10}	532	42
[Et ₄ N] ₃ [WOS ₃ (CuI) ₃ (μ_2 -I)]·H ₂ O	2.6×10^{-10}	532	43
[MoOS ₃ Cu ₂ (PPh ₃) ₃]	1.2×10^{-11}	532	44
[WOS ₃ Cu ₂ (PPh ₃) ₄]	2.0×10^{-11}	532	44
WOS ₃ Cu ₃ (SCN)(Py) ₅	8.0×10^{-11}	532	3e
MoOS ₃ Cu ₃ (SCN)(Py) ₅	2.0×10^{-10}	532	3e
[W ₂ Ag ₄ S ₈ (AsPh ₃) ₄]	1.7×10^{-10}	532	20
[Et ₄ N] ₄ [Mo ₂ O ₂ S ₆ Cu ₆]	1.6×10^{-10}	532	45
[n-Et ₄ N] ₄ [Mo ₈ Cu ₁₂ O ₈ S ₂₄]	8.2×10^{-10}	532	46
polysilane	$(1.5 \pm 0.1) \times 10^{-12}$	1064	47
porphyrin polymer	$(2.1 \pm 0.4) \times 10^{-9}$	1064	48
polyacetylene	$\sim 10^{-9}$	602	49
polythiophene	$\sim 10^{-9}$	602	50
PDA-PTS	$\sim 10^{-8}$	651	51
PDA-4BCMU	1.3×10^{-11}	1064	52
PMTBQ	4.6×10^{-9}	532	53
PPV	$\sim 4.0 \times 10^{-10}$	580, 602	54
PTS	5.0×10^{-10} to 9.0×10^{-9}	651–701	55
PDA	7.0×10^{-12}	532	56
FcC(CH ₃)=N ₂ HCS ₂ CH ₂ C ₆ H ₅	1.3×10^{-13}	308	57
Ni[FcC(CH ₃)=N ₂ HCS ₂ CH ₂ C ₆ H ₅] ₂	1.6×10^{-12}	308	57
Pd[FcC(CH ₃)=N ₂ HCS ₂ CH ₂ C ₆ H ₅] ₂	2.1×10^{-12}	308	57
Cu[FcC(CH ₃)=N ₂ HCS ₂ CH ₂ C ₆ H ₅] ₂	3.5×10^{-13}	308	57
platinum polyynes	3.1×10^{-14} to 1.0×10^{-13}	1064	58
[Co(NCS) ₂ (bpms) ₂] _n (1D)	1.07×10^{-11}	532	4a
{[Mn(NCS) ₂ (4,4'-bpy)(H ₂ O) ₂](4,4'-bpy)} _n (1D)	$< 10^{-12}$	532	4b
[HgI ₂ (4,4'-azopyridine)] _n (1D)	1.31×10^{-11}	532	59
[HgI ₂ (bpea)] _n (1D)	1.29×10^{-11}	532	59
[Pb(NCS) ₂ (bpea)] _n (1D)	1.48×10^{-11}	532	59
[Cd(en)(NO ₃) ₂ (4,4'-bpy)] _n (1D)	1.5×10^{-11}	532	60
[Zn(bbbt)(NCS) ₂] _n (1D , polymer 2)	1.62×10^{-11}	532	<i>b</i>
[Zn(pbbt)(NCS) ₂] _n (1D , polymer 3)	1.08×10^{-11}	532	<i>b</i>
[Pb(bbbm) ₂ (NO ₃) ₂] _n (2D , polymer 1)	1.67×10^{-11}	532	<i>b</i>
[Co(bbbt) ₂ (NCS) ₂] _n (2D)	2.05×10^{-12}	532	4g
[Mn(bbbt) ₂ (NCS) ₂] _n (2D)	1.27×10^{-12}	532	4g
[Cd(bbbt) ₂ (NCS) ₂] _n (2D)	1.10×10^{-12}	532	4g
[Mn(N ₃) ₂ (bbp) ₂] _n (2D)	4.78×10^{-12}	532	4h
{[Mn(NCS) ₂ (bbp) ₂ ·0.25H ₂ O]} _n (2D)	2.40×10^{-12}	532	4h
[Mn(SO ₄)(4,4'-bpy)(H ₂ O) ₂] _n (3D)	5.0×10^{-12}	532	4b
[Mn(N ₃) ₂ (4,4'-bpy)] _n (3D)	1.2×10^{-11}	532	4b

^a $\chi^{(3)}[\text{m}^2\text{V}^{-2}, \text{SI}] = (4\pi/9 \times 10^{-8})\chi^{(3)}[\text{cm}^2 \text{stat Volt}^{-2}, \text{esu}]$. bpms = 1,2-bis(4-pyridylmethyl)disulphenyl, bpy = 4,4-dipyridyl, bbbt = 1,1'-(1,4-butanediyl)bis-1*H*-benzotriazole, pbbt = 1,1'-(1,3-propylene)bis-1*H*-benzotriazole, bpea = 1,2-bis(4-pyridyl)ethane, en = ethylenediamine, bbbm = 1,1'-(1,4-butanediyl)bis-1*H*-benzimidazole, bbp = 1,3-bis(4-pyridyl)propane. ^b This work.

$10^{-19} \text{ m}^2 \text{ W}^{-1}$), and GaAs ($n_2 = -1.6 \times 10^{-17} \text{ m}^2 \text{ W}^{-1}$), and organic polymers like 4BCMU ($n_2 = 5 \times 10^{-18} \text{ m}^2 \text{ W}^{-1}$), DANS ($n_2 = 8 \times 10^{-18} \text{ m}^2 \text{ W}^{-1}$), and PTS ($n_2 = -2 \times 10^{-16} \text{ m}^2 \text{ W}^{-1}$) as measured at 1.06 and 1.31 μm .^{3b,21} Even though the n_2 values of $4.67 \times 10^{-18} \text{ m}^2 \text{ W}^{-1}$, $4.53 \times 10^{-18} \text{ m}^2 \text{ W}^{-1}$, and $3.02 \times 10^{-18} \text{ m}^2 \text{ W}^{-1}$ in this paper were obtained with $\sim 10^{-4} \text{ mol dm}^{-3}$ DMF solution, they can match those of the best known third-order NLO materials in neat solid form. Moreover, these values are also comparable to those of cluster compounds like [W₂Ag₄S₈(AsPh₃)₄] ($n_2 = 5.9 \times 10^{-17} \text{ m}^2 \text{ W}^{-1}$),²⁰ {[Et₄N]₂[MoS₄Cu₄(CN)₄]}_n ($n_2 = 1.8 \times 10^{-16} \text{ m}^2 \text{ W}^{-1}$), and {[Et₄N]₂[WS₄Cu₄(CN)₄]}_n ($n_2 = 1. \times 10^{-16} \text{ m}^2 \text{ W}^{-1}$)³ and coordination polymers like [Mn(N₃)₂(bbp)₂]_n ($n_2 = 1.21 \times 10^{-18} \text{ m}^2 \text{ W}^{-1}$), {[Mn(NCS)₂(bbp)₂·0.25H₂O]}_n ($n_2 = 6.71 \times 10^{-19} \text{ m}^2 \text{ W}^{-1}$),⁴ [Co(bbbt)₂(NCS)₂]_n ($n_2 = 5.73 \times 10^{-19} \text{ m}^2 \text{ W}^{-1}$), [Mn(bbbt)₂(NCS)₂]_n ($n_2 = 3.55 \times 10^{-19} \text{ m}^2 \text{ W}^{-1}$), and [Cd(bbbt)₂(NCS)₂]_n ($n_2 = 3.07 \times 10^{-19} \text{ m}^2 \text{ W}^{-1}$).⁴

The third-order NLO susceptibility $\chi^{(3)}$ values of polymers **1**, **2**, and **3** can be calculated from the equation $|\chi^{(3)}| = cn_0^2 n_2 / 80\pi$,²² where c is speed of light in a vacuum and n_0 is the

linear refractive index of the sample. The $\chi^{(3)}$ values are 1.67×10^{-11} esu for polymer **1**, 1.62×10^{-11} esu for polymer **2**, and 1.08×10^{-11} esu for polymer **3**. Table 4 gives the $\chi^{(3)}$ values of some known NLO materials. Compared with all the reported coordination polymers, polymers **1**, **2**, and **3** have the largest $\chi^{(3)}$ values. One notes from Table 4 that most of the well-performing NLO materials reported in the literature are conjugated organic polymers, clusters and organometallic compounds, and so on. The $\chi^{(3)}$ values of coordination polymers ranging from 1.10×10^{-12} to 1.67×10^{-11} esu are comparable to those of the known conjugated organic polymers and cluster compounds and better than those observed in organometallic compounds. The $\chi^{(3)}$ values of conjugated organic polymers are in the range 10^{-12} – 10^{-8} esu, such as $\sim 10^{-8}$ esu for PDA-PTS at 651 nm and 7.0×10^{-12} esu for PDA at 532 nm; the $\chi^{(3)}$ values of clusters range from 1.2×10^{-11} to 5.12×10^{-9} esu, such as 4.58×10^{-9}

- (21) (a) Adair, R.; Chase, L. L.; Payne, S. A. *Phys. Rev. B* **1989**, *39*, 3337. (b) Sheik-Bahae, M.; Hutching, D. C.; Hagan, D. J.; Van Stryland, E. W. *IEEE J. Quantum. Electron.* **1991**, *1*, 1296.
(22) Yang, L.; Dorsinville, R.; Wang, Q. Z.; Ye, P. X.; Alfano, R. R.; Zamboni, R.; Taliani, C. *Opt. Lett.* **1992**, *17*, 323.

esu for $\{[\text{Et}_4\text{N}]_2[\text{MoS}_4\text{Cu}_4(\text{CN})_4]\}_n$ and 2.0×10^{-11} esu for $[\text{WOS}_3\text{Cu}_2(\text{PPh}_3)_4]$, both at 532 nm; $\chi^{(3)}$ values of ferrocene derivatives vary from 1.3×10^{-13} to 2.1×10^{-12} esu. The results show that polymers **1**, **2**, and **3** possess stronger third-order nonlinear optical properties. They combine the advantage of both conjugated organic polymers and coordination compounds and will become promising candidates for NLO materials.

Through investigating the reported literature relating to the third-order NLO properties of coordination polymers, we deduct the relationships between the structures of coordination polymers and the observed NLO properties. The NLO properties of one-dimensional coordination polymers are controlled by the valence shell structures of central metal ions. Coordination polymers with open d-shell metal ions exhibit self-defocusing behaviors. Coordination polymers with d^{10} valence shell metal ions give strong self-focusing behaviors. Polymers $[\text{Co}(\text{bpms})_2(\text{NCS})_2]_n$ and $\{[\text{Mn}(\text{NCS})_2(4,4'\text{-bpy})(\text{H}_2\text{O})_2]\}_n$ with d^7 or d^5 valence shell metal ions are two examples which show self-defocusing effects. Coordination polymers $[\text{Zn}(\text{bbbt})(\text{NCS})_2]_n$, $[\text{Zn}(\text{pbtt})(\text{NCS})_2]_n$, $[\text{HgI}_2(4,4'\text{-azopyridine})]_n$, $[\text{HgI}_2(\text{bpea})]_n$, $[\text{Pb}(\text{NCS})_2(\text{bpea})]_n$, and $[\text{Cd}(\text{en})(\text{NO}_3)_2(4,4'\text{-bpy})]_n$ containing d^{10} metal ions Zn^{2+} , Hg^{2+} , Pb^{2+} , and Cd^{2+} exhibit self-focusing effects. All two-dimensional rhombohedral grid coordination polymers possess strong self-focusing effects regardless of the valence shell structures of metal ions. Polymers $[\text{Pb}(\text{bbbm})_2(\text{NO}_3)_2]_n$, $[\text{Cd}(\text{bbbt})_2(\text{NCS})_2]_n$, $[\text{Co}(\text{bbbt})_2(\text{NCS})_2]_n$, $[\text{Mn}(\text{bbbt})_2(\text{NCS})_2]_n$, $[\text{Mn}(\text{N}_3)_2(\text{bbp})_2]_n$, and $\{[\text{Mn}(\text{NCS})_2(\text{bbp})_2] \cdot 0.25\text{H}_2\text{O}\}_n$ exhibit strong self-focusing behaviors. Three-dimensional coordination polymers have the same relationships between the structures and the NLO properties as one-dimensional coordination polymers. Polymers $[\text{Mn}(\text{SO}_4)(4,4'\text{-bpy})(\text{H}_2\text{O})_2]_n$ and $[\text{Mn}(\text{N}_3)_2(4,4'\text{-bpy})]_n$ contain Mn^{2+} ion with a d^5 valence shell and show strong self-defocusing effects.

In addition, the valence shell structure of metal ions may have some influence on the strength of NLO properties. The strength can be altered by the π back-donation capacity of metal ions to ligands. The increased π back-donation capacity of metal ions to ligands may enhance the extension of the electronic π system and improve NLO properties.⁶¹ The

valence shell structures of Pb^{2+} , Co^{2+} , Mn^{2+} , Hg^{2+} , Cd^{2+} , and Zn^{2+} in Table 4 are $5d^{10}6s^2$, $3d^7$, $3d^5$, $5d^{10}$, $4d^{10}$, and $3d^{10}$, respectively, so Pb^{2+} shows the strongest electronic π back-donation capacity. In the reported two-dimensional Pb^{2+} , Co^{2+} , Mn^{2+} , and Cd^{2+} coordination polymers, the strength of NLO properties presents a regular variation to follow the decreased π back-donation capacity from Pb^{2+} to Cd^{2+} ; polymer $[\text{Pb}(\text{bbbm})_2(\text{NO}_3)_2]_n$ possesses the strongest NLO properties because the electronic π back-donation capacity of Pb^{2+} is the largest; its $\chi^{(3)}$ value is 1 order of magnitude larger than those of others two-dimensional polymers. Polymer $[\text{Cd}(\text{bbbt})_2(\text{NCS})_2]_n$ contains Cd^{2+} ion, which has a weaker electronic π back-donation capacity than Pb^{2+} , Co^{2+} , and Mn^{2+} , so the NLO properties of the polymer are the smallest.

Acknowledgment. The authors acknowledge financial support from the National Natural Science Foundation of China (20001006), Innovation Engineering Foundation of Henan Province, and Outstanding Young Teacher Foundation of Ministry of Education.

Supporting Information Available: Crystallographic data in CIF format. This material is available free of charge via the Internet at <http://pubs.acs.org>.

IC0259282

- (23) Blake, A. J.; Hill, S. J.; Hubberstey, P.; Li, W. S. *J. Chem. Soc., Dalton Trans.* **1997**, 913.
- (24) Li, M. X.; Xie, G. Y.; Gu, Y. D. *Polyhedron* **1995**, *14*, 1235.
- (25) Chen, X. M.; Tong, M. L.; Luo, Y. J.; Chen, Z. N. *Aust. J. Chem.* **1996**, *49*, 835.
- (26) Carlucci, L.; Ciani, G.; D. Proserpio, M.; Sironi, A. *J. Chem. Soc., Dalton Trans.* **1997**, 1795.
- (27) Batsanov, A. S.; Begley, M. J.; Hubberstey, P.; Stroud, J. *J. Chem. Soc., Dalton Trans.* **1996**, 1947.
- (28) Blake, A. J.; Hill, S. J.; Hubberstey, P.; Li, W. S. *J. Chem. Soc., Dalton Trans.* **1998**, 909.
- (29) Niu, Y. Y.; Hou, H. W.; Wei, Y. L.; Fan, Y. T.; Zhu, Y.; Du, C. X.; Xin, X. Q. *Inorg. Chem. Commun.* **2001**, *4*, 358.
- (30) Wu, B.; Zhang, W. J.; Yu, S. Y.; Wu, X. T. *J. Chem. Soc., Dalton Trans.* **1997**, 1795.
- (31) Bowyer, P. K.; Porter, K. A.; Rae, A. D.; Willis, A. C.; Wild, S. B. *Chem. Commun.* **1998**, 1153.
- (32) Wu, H. P.; Janiak, C.; Uehlin, L.; Klüfers, P.; Mayer, P. *Chem. Commun.* **1998**, 2637.
- (33) Otieno, T.; Rettig, S. J.; Thompson, R. C.; Trotter, J. *Can. J. Chem.* **1989**, *67*, 1964.
- (34) Otieno, T.; Rettig, S. J.; Thompson, R. C.; Trotter, J. *Can. J. Chem.* **1990**, *68*, 1901.
- (35) Jung, O. S.; Park, S. H.; Kim, D. C.; Kim, K. M. *Inorg. Chem.* **1998**, *37*, 610.
- (36) Yaghi, O. M.; Li, H.; Groy, T. L. *Inorg. Chem.* **1997**, *36*, 4292.
- (37) Losier, P.; Zaworotko, M. J. *Angew. Chem., Int. Ed. Engl.* **1996**, *35*, 2779.
- (38) Blake, A. J.; Champness, N. R.; Khlobystov, A.; Lemenovskii, D. A.; Li, W. S.; Schröder, M. *Chem. Commun.* **1997**, 2027.
- (39) Fujita, M.; Kwon, Y. J.; Sasaki, O.; Yamaguchi, K.; Ogura, K. *J. Am. Chem. Soc.* **1995**, *117*, 7287.
- (40) Lu, J.; Yu, C.; Niu, T.; Paliwala, T.; Crisci, G.; Somosa, F.; Jacobson, A. *Inorg. Chem.* **1998**, *37*, 4637.
- (41) Carlucci, L.; Ciani, G.; Proserpio, D. M. *J. Chem. Soc., Dalton Trans.* **1999**, 1799.
- (42) Chen, Z. R.; Hou, H. W.; Xin, X. Q.; Yu, K. B.; Shi, S. *J. Phys. Chem.* **1995**, *99*, 8717.
- (43) Hou, H. W.; Liang, B.; Xin, X. Q.; Yu, K. B.; Ge, P.; Ji, W.; Shi, S. *J. Chem. Soc., Faraday Trans.* **1996**, *92*, 2343.
- (44) Shi, S.; Hou, H. W.; Xin, X. Q. *J. Phys. Chem.* **1995**, *99*, 4050.
- (45) Hou, H. W.; Long, D. L.; Xin, X. Q.; Huang, X. X.; Kang, B. H.; Ge, P.; Ji, W.; Shi, S. *Inorg. Chem.* **1996**, *35*, 5363.
- (46) Shi, S.; Ji, W.; Xin, X. Q. *J. Phys. Chem.* **1995**, *99*, 894.
- (47) Kajzar, F.; Messier, J.; Rosilio, C. *J. Appl. Phys.* **1986**, *60*, 3040.
- (48) Kuebler, S. M.; Denning, R. M.; Anderson, H. L. *J. Am. Chem. Soc.* **2000**, *122*, 339.
- (49) Kajzar, F.; Messier, J. *J. Opt. Soc. Am. B* **1987**, *4*, 1040.
- (50) Logsdon, P.; Pflieger, J.; Prasad, P. N. *Synth. Met.* **1988**, *26*, 369.
- (51) Carter, G. M.; Chen, Y. J.; Rubner, M. F.; Sandman, D. J.; Thakur, M. K.; Tripathy, S. K. *Nonlinear Optical Properties of Organic Molecules and Crystals*; Academic: New York, 1987; Vol. 2, p 85.
- (52) Nunzi, J. M.; Grec, D. *J. Appl. Phys.* **1987**, *62*, 2198.
- (53) Jenekhe, S. A.; Lo, S. K.; Flom, S. R. *Appl. Phys. Lett.* **1989**, *54*, 2524.
- (54) Singh, B. P.; Prasad, P. N.; Karasz, F. E. *Polymer* **1988**, *29*, 1940.
- (55) Cater, G. M.; Thakur, M. K.; Chen, Y. J.; Hryniewicz, J. V. *Appl. Phys. Lett.* **1985**, *47*, 457.
- (56) Dennis, W. M.; Blau, W.; Bradley, D. J. *Appl. Phys. Lett.* **1985**, *47*, 200.
- (57) Tian, Y. P.; Lu, Z. L.; You, X. Z. *Acta Chim. Sin.* **1999**, *57*, 1068.
- (58) Guha, S.; Frazier, C. C.; Porter, P. L.; Kang, K.; Finberg, S. E. *Opt. Lett.* **1989**, *14*, 952.
- (59) Niu, Y. Y.; Song, Y. L.; Chen, T. N.; Xue, Z. L.; Xin, X. Q. *CrystEngComm* **2001**, *36*, 1.
- (60) Li, L. K.; Chen, B. Y.; Song, Y. L.; Li, G.; Hou, H. W.; Fan, Y. T.; Mi, L. W. *Inorg. Chim. Acta*, in press.
- (61) Chao, H.; Li, R. H.; Ye, B. H.; Li, H.; Feng, X. L.; Cai, J. W.; Zhou, J. Y.; Ji, L. N. *J. Chem. Soc., Dalton Trans.* **1999**, 3711.